Transient Electric Birefringence of N4 DNA (71 kb) in Solution

Zhulun Wang, Renliang Xu, and Benjamin Chu*

Department of Chemistry, State University of New York at Stony Brook, Long Island, New York 11794-3400. *Received March 27, 1989; Revised Manuscript Received July 26, 1989*

ABSTRACT: Field-free decays of N4 DNA (71 kb) in buffer solution have been studied by transient electric birefringence (TEB) both at high and low electric field strengths. At relatively high field strengths (0.30 kV/cm < E < 4.0 kV/cm), bimodal field-free decays were observed, in agreement with the results from the literature. The bimodal characteristics were determined by means of a regularized method of Laplace inversion (CONTIN) which did not require an a priori knowledge on the form of the decay time distribution. Our main aims in the high field strength TEB studies were (1) to show that the field-free birefringence decays for such a large DNA fragment could be nonsingle exponential and (2) to provide a reference for our low field strength TEB studies which were the main thrust of this paper. At high field strengths, both the fast and slow field-free decay times decreased slightly with increasing field strength. The faster decay time with larger amplitude reached a steady-state value whereas the slower one kept increasing with increasing pulse width. At low field strengths ($E \leq 100$ V/cm), a unimodal and extremely slow field-free decay time of the order of 10 s was observed. To our knowledge, this represents first such report on slow field-free decays of a large DNA fragment in solution. We observed that the field-free decay time increased with the pulse width and approached a steady-state value independent of the field configuration (square pulse and sinusoidal pulse) and of frequency. The steady-state field-free decay time increased with decreasing ionic strength. The higher the field strength, the shorter the pulse width needed to achieve a steady-state field-free decay time. The relaxation process at high electric field strengths might be dominated by internal motions, such as segmental orientation and internal bending, while the very long unimodal field-free decay time obtained at low field strengths might be attributed to the restoration of an entire deformed DNA molecule to its isotropic equilibrium conformation.

I. Introduction

O'Konski and Zimm[1] showed in 1950 that rotational diffusion constants of optically anisotropic molecules in solutions could be determined by transient electric birefringence (TEB) measurements. A large number of investigations on electric orientation and relaxation processes of DNA have since been reported.[2-19] At high electric field strengths ($E \geq 1$ kV/cm) and short pulse widths (≤ms), short DNA molecules (size < 300 bp) showed a single exponential field-free birefringence decay. However, multiexponential decays were found for longer DNAs.[11-17,19] The slowest relaxation time among the multidecays was mostly identified as the transverse rotational motion of the DNA molecular helix, while the faster ones might be associated with several mechansms, including segmental orienting, internal bending and twisting, and rotation of a semistiff chain.[2,11,13,16-19] The average relaxation time decreased with increasing field strength[11,17,19] or with increasing frequency by means of an applied pulsed sine-wave electric field.[4] Such relaxation time changes were attributed to the increase in the contribution of shorter segmental motions as the field strength was increased and the decrease in the contribution of longer segmental motions as the sine-wave frequency in the pulsed electric field was increased. The effect of pulse width on the relaxation time was also examined.[16,17] It was shown that a longer pulse excited slower decay modes to a larger extent relative to faster decay modes. A field-induced structural transition was observed at very high field strengths ($E \geq 10$ kV/cm).[20]

Hagerman[21] pointed out that the general conditions such as pulse width and field strength, which were needed for a whole molecule to reach orientation equilibrium, might cause substantial Joule heating. Thus, at high field strengths, TEB measurements of biological polyelectrolyte systems were restricted to short pulse widths and fluids with very low ionic strengths (~1 mM). Unfortunately, a short pulse width may not provide sufficient time to produce a steady-state orientation of an *entire* DNA chain. However, at a much lower field strength, the use of longer pulse widths in fluids with relatively low ionic strengths may provide sufficient time for the orientation of an entire DNA chain in buffer solution without appreciable Joule heating. Until now, few TEB works on DNA solutions have been reported at low field strengths.[8,9,15] Rau and Bloomfield[9] conducted TEB experiments of T7 DNA at low field strengths and observed the Kerr behavior at E < 40 V/cm. The longest relaxation time they obtained was 37 ms in 0.5 mM Na^+. A French group[8,15] observed a relatively longer relaxation time (~50 ms) at low field strengths on calf thymus DNA; but, their decay curves contained several short relaxation modes.

Theoretically, several models have been developed for calculating the rotational diffusion constant of stiff-chain macromolecules in solution. Broersma[22] suggested an expression of the rotational diffusion coefficient for a straight cylinder. Broersma's expression is quite satisfactory at large axial ratios (≥10). However, DNA molecules can be modeled as rigid cylinders only when their sizes are very small. Hearst[23] derived an expression for the rotational diffusion coefficient of stiff chains on the basis of the Kirkwood formalism. More recently, Hagerman and Zimm (HZ)[24] suggested a relationship between the rotational diffusion coefficient and the flexibility of weakly to moderately flexible chains based on the Monte Carlo analysis. The HZ approach has been applied successfully to wormlike chains with sizes up to five persistence lengths. Thus for short DNA fragments, birefringence measurements have yielded definitive information about DNA molecular structure through comparison with theoretical models for rigid or bend rods and wormlike chains. For large DNA fragments, how-

* To whom all correspondence should be addressed.

0024-9297/90/2223-0790$02.50/0

ever, the dynamic behavior cannot yet be predicted by current theoretical models.

In this study, we have examined the dynamic behavior of N4 DNA (71 kb) in buffer solution by using the TEB technique at low ionic strength, low experimental temperature, and both high and low electric field strengths with corresponding short and long pulse widths, respectively, and with either square-wave or sine-wave pulse fields. Field-free decay rates were obtained under the above conditions where the heating effect was negligible. At high field strengths and short pulse widths, the field-free decay was non single exponential and the results were in good agreement with those reported in the literature.[11-13] However, unimodal and significantly slower field-free decay times were observed when a square or sinusoidal pulse at low field strengths but over a much longer pulse duration was used. At low field strengths, we observed that the field-free decay time was able to reach a steady-state value with a long enough pulse width. We believe that the long relaxation time obtained at low field strengths is related to the restoration of anisotropic deformed DNA chain to its isotropic equilibrium conformation, not just localized segmental orientations.

This paper is organized as follows. First, we briefly introduce the TEB theory and the data analysis methods including the methods of cumulants and double exponential (DEXP) fitting as well as the CONTIN method. Second, the experimental details are discussed which include material, instrumentation, and measurement conditions. Then we present the experimental results and discussions. Finally the conclusions are given.

II. Theoretical Background

The principles of TEB have been extensively discussed by Fredericq and Houssier.[25] For a monodisperse solution of rigid axially symmetric particles, the disorientation process takes a single exponential form[26]

$$\Delta n(t) = \Delta n_0 e^{-t/\tau} \tag{1}$$

where $\Delta n(t)$ is the birefringence at time t after removal of the field, Δn_0 is the birefringence when the field is removed, and τ is the relaxation time of the particle. For a polydisperse solution or for a monodisperse solution with several modes of internal motions

$$\Delta n(t) = \sum_i \Delta n_{0,i} e^{-t/\tau_i} \tag{2}$$

For a continuous distribution, the expression becomes

$$\Delta n(t) = \int_0^\infty G(\tau) e^{-t/\tau}\, d\tau \tag{3}$$

where $G(\tau)$ is the normalized decay time distribution function.

In the present study, we have used mainly the cumulants and the DEXP fitting methods for analyzing our low field and high field field-free decay curves, respectively. In the cumulants method,[27] the cumulant expansion is given by

$$\Delta n(t) = \Delta n_0 (e^{-t/\tau + (\mu_2/2!)t^2 - (\mu_3/3!)t^3 + \dots}) \tag{4}$$

where τ^{-1} is the average decay rate and μ_i is the ith moment of the decay rate with the variance Var = $\mu_2 \tau^2$. The DEXP fitting[28] assumes that there are two decay rates. $\Delta n(t)$ is then represented by

$$\Delta n(t) = \Delta n_0 (A_1 e^{-t/\tau_1} + A_2 e^{-t/\tau_2}) \tag{5}$$

with $A_1 + A_2 = 1$ and the average decay rate $\tau^{-1} = A_1 \tau_1^{-1} + A_2 \tau_2^{-1}$. The CONTIN method[29] uses a regularization technique to seek a smooth solution for the decay rate distribution $G(\Gamma)$ with Γ being the characteristic line width and $\Gamma = \tau^{-1}$ without an a priori assumption on the form of the distribution.

Table I
Average Decay Times and Amplitudes of N4 DNA at E = 0.59 kV/cm and Pulse Width = 1.12 ms Using Different Methods of Data Analysis[a]

method	τ_1, ms	A_1	τ_2, ms	A_2
DEXP	5.8	0.29	0.59	0.71
CONTIN	5.7	0.32	0.56	0.68

[a] For DEXP, τ_1, τ_2 and A_1, A_2 are based on eq 5. For CONTIN, τ_1 and τ_2 are the average decay times as defined by $\tau_i^{-1} = \int_{\Gamma_{\min,i}}^{\Gamma_{\max,i}} \Gamma G(\Gamma)\, d\Gamma$ where $\Gamma_{\max,i}$ and $\Gamma_{\min,i}$ are the two limits of the ith peak in $G(\Gamma)$. A_1 and A_2 are the average areas under the peaks as defined by $A_i = \int_{\Gamma_{\min,i}}^{\Gamma_{\max,i}} G(\Gamma)\, d\Gamma$.

III. Experimental Section

1. Materials. A monodisperse N4 DNA fragment (71 kb) kindly provided by Dr. M. Lalande (Department of Pediatrics, Howard Hughes Medical Institute, Genetics Division, Children's Hospital, Harvard Medical School) was used in this study. The DNA stock solution (concentration = 500 μg/mL) was stored at −20 °C in Tris buffer (10 mM Tris, 1 mM EDTA, and pH 8.0). The samples used in TEB measurements were prepared by diluting the stock DNA solution with distilled deionized water to the desired concentrations. The final DNA concentration was 25 μg/mL in 0.5 mM Tris buffer and 0.05 mM EDTA or in 0.25 mM Tris buffer and 0.025 mM EDTA. The samples for TEB measurements were prepared on the day of the experiment. The overlap concentration C^* is defined as the concentration at which polymer coils begin to touch each other. For wormlike chains, C^* can be expressed by[30]

$$C^* = \frac{2^{3/2} M}{N_A (\rho L_c)^{3/2}} \tag{6}$$

with N_A, M, ρ, and L_c being Avogadro's number, the molecular weight, the persistence length, and the contour length, respectively. The influence of chain flexibility (i.e., persistence length) on the effective volume of wormlike chains has been taken into account. For N4 DNA, the value of C^* would be 160 μg/mL if a persistence length ρ of 50 nm were used. At a low ionic strength of 0.25 mM which we used, ρ was estimated to be ~100 nm from Figure 4 in ref 13. Thus $C^* \approx 58$ μg/mL. We chose the experimental concentration $C < C^*$ in order to keep the DNA molecules apart from one another and to alleviate intermolecular interactions of neighboring DNA chains. Our experimental temperature was 13.5 °C which was far away from the DNA melting temperature.

2. Instrumentation. A schematic diagram of our electric birefringence apparatus is shown in Figure 1. The following is a brief description of its components.

A 15-mW Spectra-Physics Model 124A He–Ne laser operated at λ_0 = 632.8 nm, with vertically polarized light was used as the light source. The light was focused and then polarized 45° with respect to the horizon by two Glan-Thompson polarizers. The polarizability of the light after the two polarizers can reach 99.999%. The cell assembly was composed of a 1 cm^2 Beckman cell with two platinum electrodes (0.9 cm × 0.2 cm × 5.1 cm) held by a Teflon spacer and a giant brass water-jacket whose temperature could be controlled by a Brinkmann Lauda K-2/R thermostat to ±0.05 °C. The spacing between the two electrodes was 0.3 cm. The temperature of the sample was monitored by a fast response thermistor that was embedded in the cell. After the cell, the transmitted light beam went through a quarter wave plate whose fast axis was at 45° with respect to the horizon and then through a Glan-Thompson polarizer whose axis was perpendicular to the first two polarizers.

An RCA 1P28 photomultiplier tube (PMT) and an EMI A1 preamplifier were used to convert the light signal into an electical signal which was then amplified. The resulting signal was recorded by a Gould Biomation Model 8100 dual channel recorder,

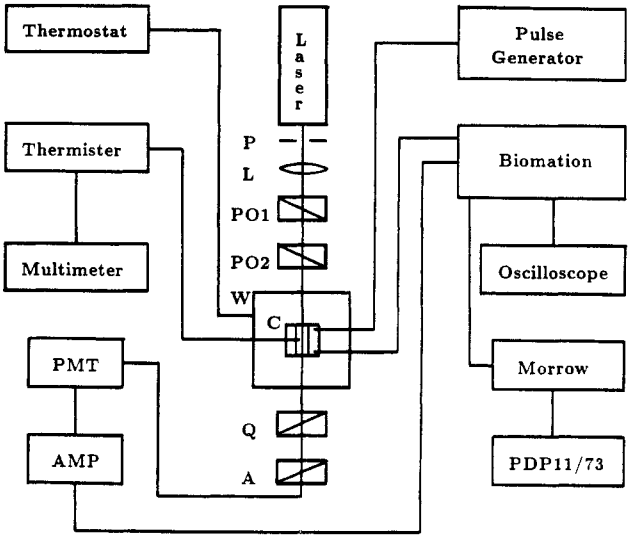

Figure 1. A schematic diagram of the TEB apparatus used in the present study: P, pinhole; L, lens; PO, polarizer; W, water jacket; C, cell; Q, $\lambda/4$ plate; A, analyzer; PMT, photomultiplier tube; AMP, amplifier. The birefringence signals could be displayed on the oscilloscope for viewing and sent to a Morrow Designs microprocessor simultaneously.

one for the electric pulse and the other for the PMT signal. The recorded data were transferred to a Morrow Designs microprocessor and then to a PDP 11-73 minicomputer for final data analysis. The data could also be displayed online on an HP 1220A oscilloscope.

For high electric fields, we used a Cober Electronics Model 605P high power pulse generator to generate high-voltage and short-pulse width square pulses. For low fields, we used a Lambda Model LL-901-OV regulated power supply and an Exact Electronics Model 120 wave form generator to generate low voltage square-wave and sine-wave pulses, respectively. The pulse width was controlled by a homemade simple circuit.

The depolarized transmitted light intensity $I(t)$ from the above set-up is derived by[25]

$$\frac{I(t)-I_s}{I_\alpha-I_s}=\frac{\sin^2(\alpha+\delta(t)/2)}{\sin^2(\alpha)} \tag{7}$$

where I_s is the instrumental stray light intensity, I_α the light intensity transmitted by the analyzer in the absence of an electic field, α an angle through which the analyzer is turned from the cross position to increase the signal-to-noise ratio and to distinguish the sign of birefringence, and $\delta(t)$ the optical retardation which is related to the birefringence by

$$\delta(t)=\frac{2\pi l\Delta n(t)}{\lambda_0} \tag{8}$$

with l and λ_0 being the path length through the solution and the wavelength of the light in vacuo, respectively. Typically, $\alpha = 0.1°$ and $I_\alpha/I_s \sim 10^3$.

A GCA/McPherson 700 Series spectrophotometer was used to monitor the denaturation of the samples.

IV. Results and Discussion

1. Hypochromicity. The melting profile of N4 DNA with a solution composition of $C_{DNA} = 25$ μg/mL, $C_{Tris} = 0.25$ mM, and $C_{EDTA} = 0.025$ mM is displayed in Figure 2. The characteristic transition temperature, also referred to as the melting temperature T_m, was about 34 °C under this condition. Since the melting temperature increases with the logarithm of the ionic strength in solution,[31] T_m at 0.5 mM Tris buffer must be higher than 34 °C. Thus, the DNA must have retained its native structure at the experiment temperature of 13.5 °C. Moreover, the UV absorbance (at $\lambda_0 = 260$ nm) remained unchanged even after a series of long pulses, indicating

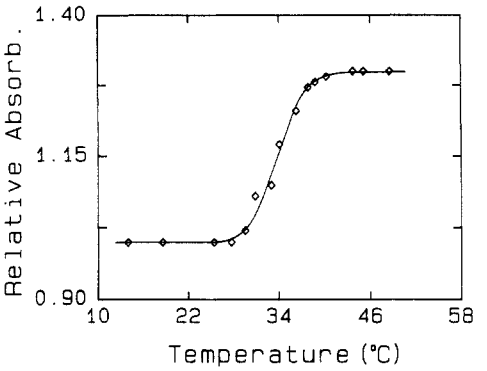

Figure 2. Melting curve of N4 DNA. DNA concentration was 25 μg/mL in 0.25 mM Tris buffer and 0.025 mM EDTA (pH 7.5). The relative absorbance was defined as the ratio of the absorbance at a temperature t to that at 25 °C. The melting temperature was determined to be about 34 °C. The DNA solution (starting at 13 °C) was brought to each (higher) temperature for about 5 min and then kept at the new temperature for about 15 min in order to establish thermal equilibrium. The whole melting curve took about 5 h.

that the pulsed electric field did not induce appreciable denaturation of the DNA double helices under our experimental conditions.

2. High Electric Field Strength. The high electric field strength covered a range of 0.30–3.8 kV/cm with corresponding short pulse widths of varying lengths from 0.03 to 3 ms. Under this condition, we observed that the field-free decay was not a single exponential, which was in agreement with other literature results.[13] It is known that even for rigid bodies the birefringence decay curves may contain up to five exponential relaxation times.[32] Furthermore, the orientation of different DNA segments could be coupled to the overall internal motions making the birefringence decay curve more complex. A typical high field birefringence signal is shown in Figure 3a. Our high field data could be well-fitted to a double exponential form as shown in Figure 3b. However, we did not assume the bimodal characteristics of our observed decay curves. First, the CONTIN yielded a bimodal decay rate distribution whose average decay rates and amplitudes agreed with those determined by the DEXP fitting procedures as shown typically in Figure 3c. Thus, we took the bimodal characteristics of our birefringence curve as confirmed experimentally by using the CONTIN method.

Figure 4 shows the field strength dependence of field-free relaxation times, τ_1 and τ_2, extracted from the DEXP fitting with a constant pulse width of 0.3 ms. The apparent relaxation times decrease with increasing field strength, in agreement with earlier findings.[2,4,16,17] The relaxation time which reflects the orientation of an entire DNA chain should be independent of the electric field strength if the macromolecular conformation were to remain constant. Stellwagen[11] and Hagerman[13] observed that the rotational relaxation time for short DNAs (size < 250 bp) could be independent of applied field strengths. The high field, associated with only short pulse widths due to the limitation of the Joule heating effect, could initiate the orientation of entire short DNA chains which already reached a steady-state deformation under those applied field strengths. However, the high field strengths/short pulse width arrangements were not able to orient an entire large DNA chain to a steady-state value during the orientation process. There were various interpretations on the multiexponential decay modes observed in birefringence decay curves of flexible DNAs. Golub[2]

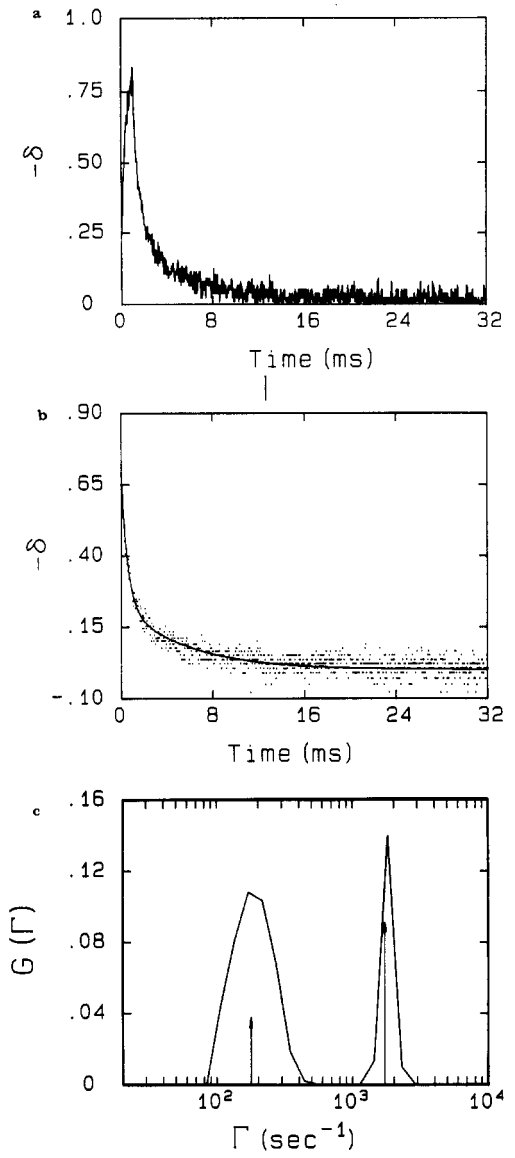

Figure 3. a. A typical high field birefringence trace for N4 DNA. The field strength was 0.59 kV/cm, and the pulse width was 1.12 ms, with a DNA concentration C_{DNA} of 25 μg/mL in 0.5 mM Tris buffer and 0.05 mM EDTA, at 13.5 °C. b. The same field-free birefringence decay curve (dots) of N4 DNA in a high field as in a. The solid curve represents a DEXP fit with the parameters listed in Table I. c. A bimodal decay rate distribution $G(\Gamma)$ from the CONTIN analysis of N4 DNA using the same high field field-free decay curve as in b. The results of the CONTIN fit are also listed in Table I. Two vertical arrow lines represent two decay rates from the DEXP fitting.

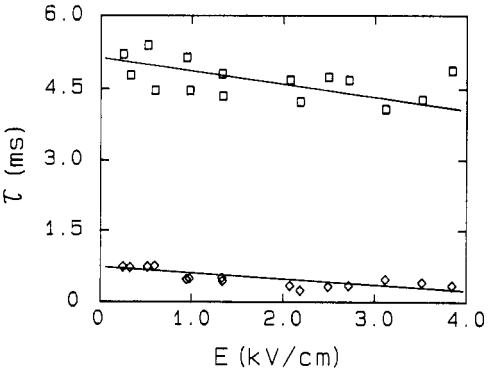

Figure 4. The field strength dependence of relaxation times of N4 DNA at high field strengths. The pulse width was 0.30 ms. The solution composition was the same as that in Figure 3a. The hollow squares and diamonds denote the two relaxation times τ_1 and τ_2 from the DEXP fitting, respectively.

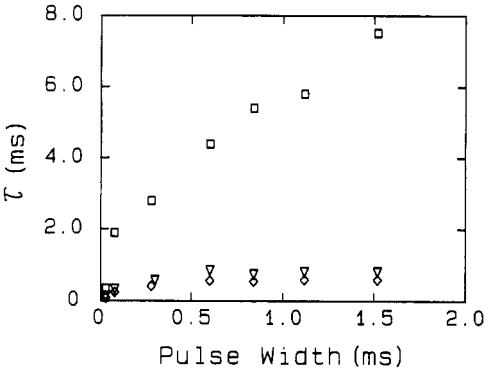

Figure 5. The dependence of relaxation times on the pulse width. The hollow squares, diamonds, and inverse triangles denote τ_1, τ_2, and τ^{-1} (= $A_1\tau_1^{-1} + A_2\tau_2^{-1}$) from the DEXP fitting, respectively. The conditions were the same as those in Figure 3a.

suggested that the relaxation pocesses were due to the orientation of molecular segments, not due to the rotation of the entire molecule because the sections of the molecule, which were sufficiently apart for a flexible DNA, would orient independently in an electric field. Stellwagen[11] attributed the observed short relaxation components to the internal bending or twisting motion or the motions associated with the return of the stretched DNA molecules to their equilibrium conformations. She also attributed the long relaxation mode that were independent of the field strength to the motion of the whole DNA chain. Hagerman[13] indicated that the average relaxation time could represent a weight average of the segmental motions and overall orientation. More recently, Lewis et al.[16,17] demonstrated that they could separate the multidecay process by the same CONTIN analysis which we used. They designated the slowest decay mode as the rotational motion of the molecule, the next faster mode as the rotation of a semistiff polymer chain equivalent to half of the overall length of the DNA chain and the even faster modes as the internal bending of the DNA chain. Furthermore they pointed out that the slowest mode might involve a coupling of rotational and bending motions for flexible DNAs. Also, Diekmann et al.[19] postulated that the coupling between orientation and bending might exist for large DNAs. According to our experiments, a bimodal decay process was observed for a very long DNA fragment with monodisperse size at high field strengths. Both relaxation modes depended on the field strength. We performed the TEB measurements at high field strengths in order to establish a reference for our experiments at low field strengths; i.e., with our experimental setups we obtained similar results as those reported in the literature.

Figure 5 shows the dependence of the relaxation times upon pulse width at a high field strength (E = 0.59 kV/cm). The average relaxation time τ is $(A_1\tau_1^{-1} + A_2\tau_2^{-1})^{-1}$ from the DEXP fitting. The fast component τ_2 dominated the whole relaxation process. As the pulse width was increased, both the short relaxation time τ_2 and the average one τ seemed to approach plateau values but the slower relaxation time (τ_1) kept increasing. Thus at high field strengths, a short pulse width was able to activate the overall orientation even though it was not enough to fully orient and deform the entire large DNA chain to some steady-state value. The longer pulse width could initiate larger segmental orientations and cause the relaxation time to increase if this relaxation process was dom-

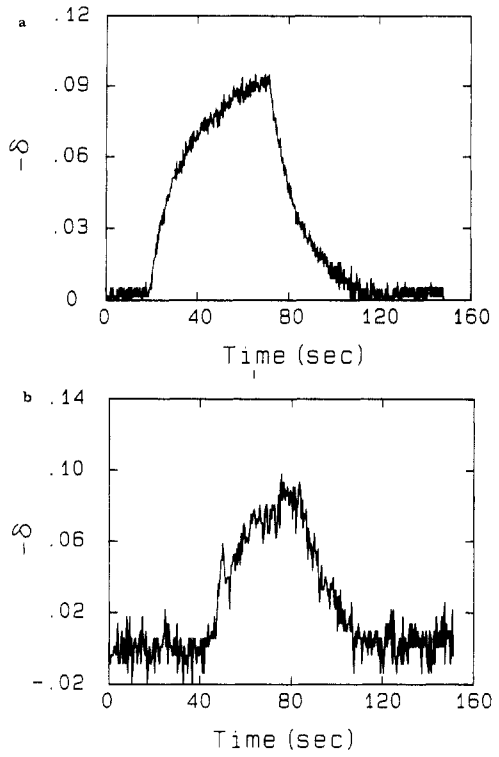

Figure 6. a. A typical pulsed sine-wave low field birefringence trace of N4 DNA. The field strength was 36 V/cm with a frequency of 10 kHz and a pulse width of 51 s. The solution composition was the same as that in Figure 3a. b. The noisy birefringence signal in a square-wave pulse field. The field strength was 36 V/cm with a pulse width of 41.2 s. The solution composition was the same as that in Figure 3a.

inated by segmental orientation. The relaxation time never reached a plateau value due to the limitation of applied pulse widths, which implied that we were not observing the overall chain relaxation. To the best of our knowledge, there are few reported TEB experiments on large DNAs (≥71 kb) in solution. Furthermore, the experimental conditions, such as ionic strength, field strength, pulse width, concentration, and temperature, etc., were very different. Thus, it is not practical to compare our results exactly with the literature results. But the range of our field-free relaxation time (≈ms) is consistent with those in references.[2,4,13]

3. Low Electric Field Strength. Our low field TEB measurements were conducted at electric field strengths $E \leq 100$ V/cm with pulse widths up to 77 s. Both square-wave and sine-wave pulses were applied. Two frequencies, 10 kHz and 100 Hz, were used in the case of sinusoidal fields. Two ionic strengths, about 0.5 and 0.25 mM, were tested. The resistance of the sample solution was about 1 MΩ. The low ionic strength and the low field strength allow longer pulse width without perturbation of the Joule heating effect. For the long pulse-width experiments, the temperature rise due to Joule heating was measured to be ≤0.1 °C by using the low ionic strength buffer solutions of the present study. Blank tests were also made; i.e., low field strengths and long pulse widths were applied to buffer solutions without DNAs, and no birefringence signals were observed. At low field strengths, the observed field-free decay appeared to be unimodal. Thus, the field-free decay was analyzed by the cumulants fitting procedure. Very long relaxation times (of the order of ten seconds) with small variances were observed. The rise curve had a similar behavior as shown in Figure 6a.

Table II
Relaxation Times of N4 DNA in Pulsed Sine-Wave Fields[a]

freq	pulse width, s	τ, s
10 kHz	77.0	14.0
	51.0	14.3[b]
	36.8	14.2
	18.3	11.6
	3.6	6.1
	2.0	2.7
100 Hz	77.0	14.4
	54.0	13.9
	35.8	13.0
	17.2	11.1

[a] DNA concentration was 25 μg/mL in 0.5 mM Tris buffer and 0.05 mM EDTA. The electric field strength E was 36 V/cm, and the temperature was 13.5 °C. [b] The field-free decay time (τ = 14.3 s) and the rise time (τ_Γ = 13.5 s) are comparable as shown in Figure 6a. The variance ($\mu_2\tau_2$) from a second-order cumulant fit are Var (field-free decay) = 0.04 and Var (rise curve) = 0.02. Thus, "single" exponential behavior dominates both the rise and decay curves at E = 36 V/cm.

3.1. Square-Wave and Sine-Wave Pulse Electric Field. At very low field strengths ($E \leq 36$ V/cm), we found that the signal-to-noise ratio was much higher by using a pulsed sine-wave field than that by using a pulsed square-wave field. Parts a and b of Figure 6 show the observed birefringence signals by using a sinusoidal pulse field and by using a square pulse field, respectively. In the case of sine waves, neither signal averaging nor curve smoothing, the common methods used in birefringence experiments for treating noisy data, was needed. We analyzed the field-free decay directly by the cumulants fitting procedure. In the case of square waves, the noisy data was pretreated by a software low-frequency pass-filtering technique[33] and then analyzed by means of the cumulants method. By comparing the fitting results from raw data with those from pretreated data, we found that the high-frequency noise resulted in only a large apparent variance but did not affect the relaxation time. Comparable results were obtained from both sinusoidal and square pulse field birefringence measurements. We have used a very fast frequency, 10 kHz, and a much slower one, 100 Hz, in the pulsed sine-wave field. The obtained birefringence amplitudes and field-free relaxation times were identical at these two frequencies. The relaxation times of varying pulse widths at these two frequencies are listed in Table II.

We had to apply the pulse for quite a long time (~tens of seconds) in order to achieve a steady-state amplitude of the birefringence at low fields. Therefore, the effects due to the polarization of electrodes should be considered. The use of a train of sine waves or of pulses of alternating signs should reveal the existence of the polarization effect. It is well-known that the counterion atmosphere has a severe effect on the static and dynamic properties of polyions. It has been proposed that the induced polarized counterion atmosphere contributes significantly to the overall orientation of the DNA chain.[1,34] However, at much higher frequencies, the counterion atmosphere polarization is expected to be less important.[35] Under the present conditions of very low field strengths and high frequency (10 kHz), the counterion atmosphere polarization cannot follow the rapid alternating field. As the observed birefringence relaxation time was independent of the field configuration (square pulse or sinusoidal pulse) and frequency, the electrode and counterion atmosphere polarization could not have an appreciable effect on the relaxation process.

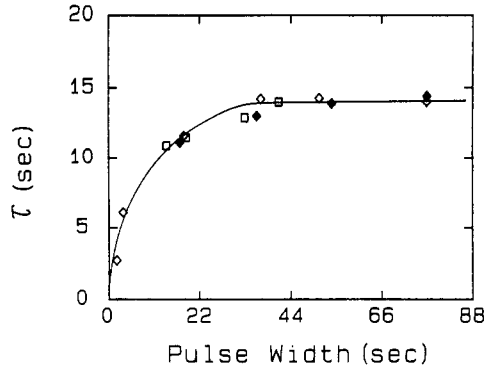

Figure 7. The pulse width dependence of relaxation times in a low field with E = 36 V/cm. The hollow squares denote the τ in a square-wave pulse field. The hollow and filled diamonds denote the τ in a pulsed sine-wave field with frequencies of 10 kHz and 100 Hz, respectively. The relaxation time τ was from the cumulants fitting. The solution composition was the same as that in Figure 3a.

3.2. Pulse Width Dependence and Field Strength Dependence. Figure 7 shows the pulse width dependence of the birefringence relaxation times from the field-free decays of the pulsed sine-wave (two frequencies) field and the pulsed square-wave field. The relaxation time increased with increasing pulse width and finally reached a plateau value of ~14 s. It should be noted that when the pulse width is long enough to yield a steady-state field-free relaxation time, the amplitude of birefringence has also reached its steady state. To our knowledge, such a long birefringence relaxation time has not been reported before. First of all, we used large monodisperse DNA (size ~ 71 kb) chains that were sufficiently flexible for its segments to be oriented independently in addition to its overall deformation in an electric field. When a large DNA molecule is subjected to a short pulse width at high field strengths, the pulse duration would be too short to deform appreciably the conformation of an entire chain, or even if the deformation of the overall chain conformation did occur, the overall deformation could not reach a steady-state anisotropic conformation. However, at low field strengths, the pulse width could be applied sufficiently long to induce a steady-state deformation for the whole DNA chain. Segmental and rotational motions could also occur during this pulse time, and they should be coupled to the overall chain deformation. For example, we used a very long pulse width (up to ~77 s) at a low pulsed sine-wave field with E ~ 36 V/cm. We observed a steady-state birefringence value of a very long relaxation time (~14 s) with a small variance (<0.05). Furthermore, the steady-state relaxation time is relatively independent of the applied electric field strength over the range of 36 and 100 V/cm. We suggest that the field-free decay is due to the restoration of deformed anisotropic DNA chain to its equilibrium, isotropic conformation.

We have carried out the experiments at three relatively low field strengths in order to examine the field strength effect. The relaxation times at different electric field strengths with different pulse widths are listed in Table III. The higher the electric field strength, the shorter the pulse width needed for obtaining the steady-state relaxation time. We observed that the steady-state relaxation times were the same at different field strengths.

3.3. The Effect of Ionic Strength. A double-helical DNA molecule becomes a wormlike chain at sufficiently long chain length. It has been suggested that over a short range of lengths DNAs are rodlike, but over the entire length of the molecule, they curve and bend in arbitrary directions.[36] The persistence length ρ represents the stiffness of the wormlike chain. The persistence length increases with decreasing ionic strength. Thus, the electrooptical properties of DNA are sensitive to ionic strength. When the ionic strength is above 1 mM, the dependence of the persistence length upon the ionic strength is not so evident. But when the ionic strength is below 1 mM, this effect is quite pronounced.[13] Great chain expansion and thus large persistence lengths have been reported at various salt concentrations.[37] We conducted another set of birefringence experiments at 0.25 mM Tris buffer under a pulsed sine-wave field of the field strength 100 V/cm and frequency 10 kHz. The observed field-free steady-state relaxation time was 21 s which was longer when compared with the τ value of 14 s at 0.5 mM Tris buffer. The decrease in the ionic strength causes a decrease in the flexibility of the DNA chain and, therefore, an increase in the disorientation time.

Table III
Relaxation Times of N4 DNA in Square-Wave Pulse Fields[a]

field strength, V/cm	pulse width, s	τ, s
36	41.2	14.0
	33.0	12.9
	18.8	11.5
	14.0	10.9
68	7.2	12.5
100	8.2	14.4
	6.2	13.6
	5.0	9.8

[a] DNA concentration was 25 μg/mL in 0.5 mM Tris buffer and 0.05 mM EDTA. The experimental temperature was 13.5 °C.

3.4. Comparison with Theoretical Models. According to Broersma,[22] the rotational diffusion coefficient D_R of a straight cylinder is given by

$$D_{R,B} = \frac{3k_BT}{\pi\eta_0 L^3}\{\ln(L/b) - 1.43 + 7[1/\ln(L/b) - 0.27]^2\} \quad (9)$$

with k_B, T, η_0, L, and b being the Boltzmann constant, the absolute temperature, the viscosity of the solvent, the axial length, and the radius of the cylinder, respectively. The decay time for noninteracting rigid particles of cylindrical symmetry is related to the rotational diffusion constant by[38]

$$\tau = 1/(6D_R) \quad (10)$$

If we assume that the DNA molecule was fully extended to a rod with b = 1.3 nm,[36] $L = L_c$ = 24 μm; and L_c, the contour length, we obtained the transverse rotational relaxation time of a straight cylinder τ_B = 71 s according to eq 9 and eq 10.

As an alternative model, Hearst[23] derived an expression for the rotationary constant of a long wormlike chain. In a bead model[24]

$$D_{R,H} = \frac{k_BT}{\eta_0}\left(\frac{\lambda}{a}\right)^3\left(\frac{1}{n\lambda}\right)^2[0.253(\lambda n)^{1/2} + 0.159\ln(1/\lambda) - 0.227] \quad (11)$$

where $\lambda = a/(2\rho)$ and $n = (N-1)/2$, with a and N being the distance between the frictional elements and the number of elements, respectively. If we took $\rho \approx 100$ nm and $a \approx 3.2$ nm,[39] we obtained τ_H = 0.51 s.

In the HZ approach,[24] a pertinent quantity R (= τ_W/τ_B with τ_W being the longest rotational relaxation time of a wormlike chain and $\tau_B = 1/(6D_{R,B})$ determined from eq 9) was introduced. The relationship between R and

the reduced contour length L_c/ρ was derived on the basis of the equilibrium–ensemble approach. Without assuming configuration preaveraging, the HZ model provides a more precise information about the hydrodynamic properties of flexible polymers. Within the valid range of their model ($0.1 < L_c/\rho < 5$), the R value ($1.0 > R > 0.3$) from their analysis is larger than the R calculated from the Hearst long wormlike chain model, indicating that the relaxation time τ of a wormlike chain from the more precise HZ model should be larger than that from the Hearst wormlike chain model. On the basis of our experimental observation, our $\tau \approx 14$ s is much larger than $\tau_H = 0.51$ s calculated from the Hearst wormlike chain model. Since our L_c/ρ value is out of the valid range of the HZ model, it is difficult to compare our R value with that from their model exactly. However, our R is smaller than the lower limit of $R \sim 0.3$ of the HZ model; since our L_c/ρ is larger than the upper limit of $L_c/\rho \sim 5$ and is larger than R_H, the tendency is consistent with the HZ model.

Doi and Edwards have predicted that the rotational diffusion coefficient of rodlike polymers in the semidulute regime has a C^{-2} dependence.[41] Hence, the relaxation time τ is proportional to C^2. This dependence has been demonstrated by other experiments.[42] In order to check whether the observed long relaxation time was due to intermolecular interactions, especially as a result of extended coil entanglement, we also made measurements at two other DNA concentrations, 20 and 30 μg/mL. The measured relaxation times were independent of DNA concentrations. Therefore, we concluded that our experiments were performed in the dilute solution regime.

Yanagida et al.[40] reported their observation of DNA conformation in solution by fluorescence microscopy. In the absence of external forces, DNA molecules in solution fluctuated among three conformations, i.e., sphere, ellipsoid, and flexible rod, rapidly. However, the DNA chains were extended to thick filaments and aligned by external force (water stream). The thick filaments could be further elongated into thin filaments by solvent flow. The filaments shortened back when the external force was removed. The transition time was in the second range. Here, we have τ_H (≈ 0.51 s) $< \tau$ (≈ 14 s) $< \tau_B$ (≈ 71 s), indicating that the DNA conformation is closer to an extended chain under the present experimental conditions of low electric fields and long pulse widths. Our long field-free decay should represent the restoration of an elongated chain to its equilibrium conformation.

V. Conclusions

In summary, the high field strength TEB experiments of very large DNAs demonstrate that the field-free decay time is nonunimodal. At high field strengths and short pulse widths, it seems quite reasonable to use the double exponential method for N4 DNA in buffer solution, as supported by experimental observations and confirmed by the CONTIN analysis. The field strength and pulse width dependences of the relaxation times indicate that the internal motions, such as segmental orientations and internal bending, may be dominant instead of the overall DNA molecular orientation, as the pulse width is too short to orient a whole large DNA molecule. However, at low field strengths with long pulse widths unimodal field-free decays were observed. The relaxation time could achieve a steady-state value which increases with decreasing ionic strength. The steady-state relaxation time shows no field configuration (square pulse or sinusoidal pulse) and frequency dependences. In comparison with theoretical models, this kind of relaxation time is closer to that of a deformed anisotropic DNA chain instead of a unperturbed wormlike chain. The observation is consistent with the fluorescence microscope observation of DNA thick filament conformations under an external force. The elongation of the DNA chain by the electric field takes place during the long pulse duration. Therefore the observed long relaxation time could be reasonably attributed to the restoration of an entire deformed DNA chain to its isotropic equilibrium conformation.

Acknowledgment. Many thanks to Dr. M. Lalande for providing us the DNA sample and to Professor B. H. Zimm for suggesting to us the use of sinusoidal fields. This research was supported by the Polymers Program of the National Science Foundation (DMR8617820).

References and Notes

(1) O'Konski, C. T.; Zimm, B. H. *Science* **1950**, *111*, 113.
(2) Golub, E. I. *Biopolymers* **1964**, *2*, 113.
(3) Hornick, C.; Weill, G. *Biopolymers* **1971**, *10*, 2345.
(4) Miller, S. J.; Wetmur, J. G. *Biopolymers* **1974**, *13*, 115.
(5) Colson, P.; Houssier, C.; Fredericq, E. *Biochim. Biophys. Acta* **1974**, *340*, 244.
(6) Greve, J.; de Heij, M. E. *Biopolymers* **1975**, *14*, 2441.
(7) de Groot, G.; Greve, J.; Blok, J. *Biopolymers* **1977**, *16*, 639.
(8) Roux, B.; Bernengo, J.-C.; Marion, C. *J. Colloid Interface Sci.* **1978**, *66*, 421.
(9) Rau, D. C.; Bloomfield, V. A. *Biopolymers* **1979**, *18*, 2783.
(10) Yamaoka, K.; Matsuda, K. *Macromolecules* **1980**, *13*, 1558.
(11) Stellwagen, N. C. *Biopolymers* **1981**, *20*, 399.
(12) Elias, J. G.; Eden, D. *Macromolecules* **1981**, *14*, 410.
(13) Hagerman, P. J. *Biopolymers* **1981**, *20*, 1503.
(14) Elias, J. G. Ph.D. Thesis, Yale University, 1981.
(15) Marion, C.; Perrot, B.; Roux, B.; Bernengo, J. C. *Makromol. Chem.* **1984**, *185*, 1665.
(16) Lewis, R. J.; Pecora, R.; Eden, D. *Macromolecules* **1986**, *19*, 134.
(17) Lewis, R. J.; Pecora, R.; Eden, D. *Macromolecules* **1987**, *20*, 2579.
(18) Ding, D.-W.; Rill, R.; van Holde, K. E. *Biopolymers* **1972**, *11*, 2109.
(19) Diekmann, S.; Hillen, W.; Morgeneyer, B.; Wells, R. D.; Porschke, D. *Biophys. Chem.* **1982**, *15*, 263.
(20) O'Konski, C. T.; Stellwagen, N. C. *Biophys. J.* **1965**, *5*, 607.
(21) Hagerman, P. J. *Methods Enzymol.* **1985**, *117*, 198.
(22) Broersma, S. *J. Chem. Phys.* **1960**, *32*, 1626; *J. Chem. Phys.* **1981**, *74*, 6989.
(23) Hearst, J. E. *J. Chem. Phys.* **1963**, *38*, 1062.
(24) Hagerman, P. J.; Zimm, B. H. *Biopolymers* **1981**, *20*, 1481.
(25) Fredericq, E.; Houssier, C. *Electric Dichroism and Electric Birefringence*; Clarendon Press: Oxford, UK, 1973.
(26) Benoit, H. *J. Chim. Phys.* **1951**, *48*, 612.
(27) Koppel, D. E. *J. Chem. Phys.* **1972**, *57*, 4814.
(28) Chu, B.; Ford, J. R.; Dhadwal, H. *Methods Enzymol.* **1985**, *117*, 256.
(29) Provencher, S. W. *Makromol. Chem.* **1979**, *180*, 201.
(30) Ying, Q.; Chu, B. *Macromolecules* **1987**, *20*, 362.
(31) Bloomfield, V. A.; Crothers, D. M.; Tinoco, I., Jr. *Physical Chemistry of Nucleic Acids*; Harper & Row: New York, 1974.
(32) Wegener, W. A.; Dowben, R. M.; Koester, V. J. *J. Chem. Phys.* **1979**, *70*, 622.
(33) Arsenault, H. H.; Marmet, P. *Rev. Sci. Instrum.* **1977**, *48*, 512.
(34) Rau, D. C.; Charney, E. *Biophys. Chem.* **1983**, *17*, 35.
(35) O'Konski, C. T.; Haltner, A. J. *J. Am. Chem. Soc.* **1957**, *79*, 5634.
(36) Cantor, C. R.; Schimmel, P. R. *Biophysical Chemistry*; W. H. Freeman: San Francisco, 1980; Part III.
(37) Harrington, R. E. *Biopolymers* **1978**, *17*, 919.
(38) Benoit, H. *Ann. Phys.* **1951**, *6*, 561.
(39) Garcia de la Torre, J.; Bloomfield, V. A. *Biopolymers* **1977**, *16*, 1747.
(40) Yanagida, M.; Hiraoka, Y.; Katsura, I. *Cold Spring Harbor Symp. Quant. Biol.* **1982**, *47*, 177.
(41) Doi, M. *J. Phys. (Les Ulis, Fr.)* **1975**, *36*, 607. Doi, M.; Edwards, S. F. *J. Chem. Soc., Faraday Trans. 2* **1978**, *74*, 560.
(42) For example, Zhou, Z.; Georgalis, Y.; Liang, W.; Li, J.; Xu, R.; Chu, B. *J. Colloid Interface Sci.* **1987**, *116*, 473.